International Journal of Mechanics and Energy (IJME)
Vol. 2, Issue 2, 2014, ISSN: 2286-5845

Simulation of a solar driven ammonia-water absorption refrigeration system

Yasmina Boukhchana*, Ali Fellah, Ammar Ben Brahim

Research Unit: Applied Thermodynamics (UR:11ES80), National School of Engineers of Gabes (ENIG), University of Gabes, Omar Ibn El Khattab sreet, 6072 Gabes, TUNISIA

Abstract: A steady state computer simulation model has been developed to predict the performance of an absorption refrigeration system using NH_3-H_2O as a working pair and driven by solar energy. It satisfies the air-conditioning supplies of a classroom. The absorption system includes an absorber, a generator, a condenser, an evaporator and a liquid heat exchanger. It uses a solar collector to achieve the thermal necessities of the vapor generator. The model is based on detailed mass and energy balances and heat and mass transfer relationships. The effects of the coefficient of performance and effectiveness of heat exchangers on the key operational parameters are investigated. To eliminate the numerical errors, thermodynamic properties of the working pair are taken from the EES software. The results show that the COP of the system can reach a value greater than 0.4. The effectiveness increase leads to an increase in COP of about 55%.

Key words: Solar energy, Absorption refrigeration, Ammonia-water, Simulation, COP.

1. Introduction

Energy is considered as a major agent in the generation of wealth and an important factor in economic development. With developing technology, the rapid increase in the population of the world, life standards and comfort demands in conjunction with architectural characteristics and trends, the demand for energy and its use for cooling are ever increasing [1]. In a world of continuously growing scarcity of primary energy as well as of an insurmountable irreversible environmental impact, due to human activity onto the biosphere, it is of utmost importance to look for alternatives to traditional energy sources [2]. The main advantages concern the reduction of peak loads for electricity utilities, the use of zero ozone depletion impact refrigerants, the decreased primary energy consumption and decreased global warming impact [3]. In summer, particularly under tropical climate, air conditioning has the highest energy expenditure in buildings [4]. During recent years, research aimed at the development of technologies that can offer reductions in energy consumption, peak electrical demand, and energy costs without lowering the desired level of comfort conditions has been intensified. Alternative cooling technologies that can be applied to residential and commercial buildings, under a wide range of weather conditions, are being developed [5].

For refrigeration field, the reduction of energy consumption cannot be relied solely on the improvement of efficiency. Solar cooling is without a doubt an interesting alternative for solving problems of electrical overconsumption in traditional compression vapor air conditioning. Solar energy usage for cooling purpose offers the advantage of using an inexhaustible and free heat source to meet cooling needs most of the time [4, 6]. Considering that cooling demand increases with the daily maximum intensity of solar radiation, solar refrigeration has been considered as a logical solution [7].

Solar energy occupies one of the most important places among various alternative energy sources [8]. In

***Corresponding author:** Yasmina Boukhchana
E-mail: Yasmina.Boukhchana@enig.rnu.tn.

particular, it has been identified as a convenient renewable energy source, because it is more widely available and can be stored in batteries via photovoltaic (PV) arrays, and converted to heat or mechanical energy with reasonable efficiency [9]. The direct use of solar energy as primary energy source is interesting because of its universal availability and low environmental impact. Different technologies can be adopted to get refrigeration from solar energy: thermal and electric solar systems, and some new emerging technologies. The solar thermal systems include absorption, adsorption, solar ejector, thermo-mechanical and regenerative desiccant solutions [10]. Absorption cooling has been one of the first and oldest forms of air conditioning and refrigeration systems since it was invented in eighteen century. Absorption systems are thermally activated, and they do not require high input shaft power. Therefore, where power is unavailable or expensive or where there is waste, geothermal, or solar heat available, absorption machines could provide reliable and quiet cooling. As no chlorofluorocarbons (CFCs) are used, absorption systems are friendlier with the environment [11-13]. In addition, they do not contribute to the ozone depletion or to global warming [14, 15]. Although absorption systems seem to provide many advantages, its COP is too low and its investment cost is very expensive [16, 17]. The most usual combinations of fluids include lithium bromide-water (LiBr-H_2O), where water vapor is the refrigerant, and ammonia-water (NH_3-H_2O) systems, where ammonia is the refrigerant [18-20].

Based on the cooling temperature demand, the applications of solar absorption systems can be broadly classified into three categories: air-conditioning (8–15°C) for spaces, refrigeration (0–8 °C) for food and vaccine storage [19]. In this section, the development of solar absorption refrigeration systems is presented and researches currently in progress for different applications are also discussed. In the 1960s, solar-powered absorption systems were considered to be used in the field of air-conditioning [21, 22]. The first large-scale experiments for air-conditioning can be traced to 1970s. In 1976 around 500 solar-powered air-conditioning systems were installed in USA, most of which were absorption systems using LiBr [19]. Yeung et al. [23] designed and constructed a solar-powered absorption air-conditioning system to study the feasibility of utilizing solar power for comfort cooling in Hong Kong. The system consisted of a flat-plate collector array with a surface area of 38.2m^2, a 4.7kW nominal cooling capacity H2O-LiBr absorption chiller, a 2.75m^3 hot-water storage tank, a cooling tower, a fan-coil unit, an electrical auxiliary heater. It had an annual system efficiency of 7.8% and an average solar fraction of 55%. Syeda et al. [24] studied a solar cooling system for typical Spanish houses in Madrid. The system consisted of a flat-plate collector array with a surface area of 49.9m^2, a 35 kW nominal cooling capacity single-effect (H2O–LiBr) absorption chiller. This machine operated within the generation and absorption temperature ranges of 57-67°C and 32-36°C, respectively. The measured maximum instantaneous, daily average and period average COP were 0.6 (at maximum capacity), 0.42 and 0.34, respectively. Assilzadeh et al. [25] presented a H_2O–LiBr absorption unit using evacuated tube solar collectors for Malaysia and similar tropical regions. After the modeling and simulation carried out with TRNSYS program, the author concluded that the optimum system for Malaysia's climate for a 3.5kW system consists of 35m^2 evacuated tubes solar collector sloped at 20°C.

Various kinds of solar absorption refrigerators have been developed for refrigeration purpose. Uppal et al. [26] built in 1986 a small capacity (56 l) solar-powered NH_3–H_2O absorption refrigerator to store vaccines in remote locations. In the same period, Staicovici [27] developed an intermittent single-stage solar absorption system for fish preservation. Actual thermal COP of 0.25–0.30 could be achieved at generation and condensation temperatures of 80 and 24.31°C,

respectively. In 1993, Sierra et al. [28] used a solar pond to power an intermittent absorption refrigerator with NH_3–H_2O solution. It is reported that generation temperatures as high as 73°C and evaporation temperatures as low as -2°C could be obtained. The thermal COP working under such conditions was in the range of 0.24–0.28. Hammad and Habali [29] designed a solar-powered absorption refrigeration cycle using NH_3–H_2O solution to cool a vaccine cabinet in the Middle East. A year round simulation indicated that thermal COP ranged between 0.5 and 0.65 with generation temperature at 100–120°C and the cabinet inside temperature at 0–8°C. In 2001, De Francisco et al. [30] developed and tested a prototype of 2 kW NH_3–H_2O absorption system in Madrid for solar-powered refrigeration in small rural operations. The test results showed unsatisfactory operation of the equipment with COP lower than 0.05.

In the present study, a modeling of a solar absorption refrigeration system using a flat-plate collector and NH_3-H_2O pair is analyzed regarding the mass and energy balance in each component.

2. Description of the system

The term strong solution refers to a solution with a high refrigerant content. In the same way, when a weak solution is mentioned, it is understood to mean a solution with a low content of refrigerant. For this system, ammonia is the refrigerant and water is the absorbent. The water presents a vapor pressure that is not negligible compared to that of ammonia. Thus the vapor raised in the generator contains a certain amount of water. This would negatively affect the performance of the entire cycle. To reduce the water content in the refrigerant flow, a separator is typically used.

The simulated absorption refrigeration system consists of four basic components: an absorber, a generator, a condenser and an evaporator, as shown schematically in Fig. 1.

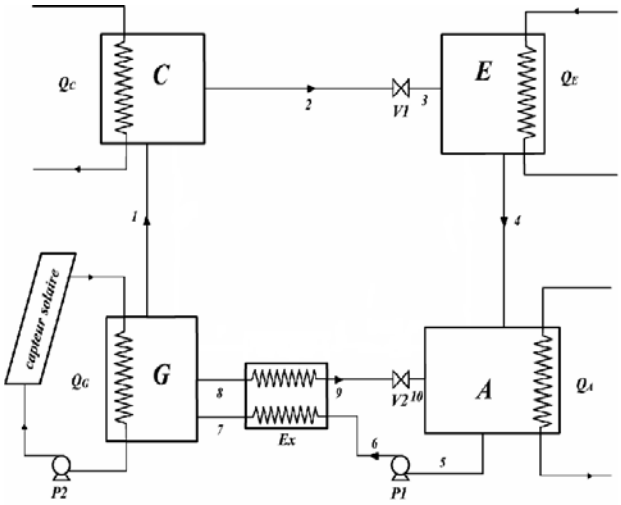

Fig. 1 Schematic of absorption refrigeration cycle.

An economizer heat exchanger, placed between the absorber and the generator, makes the process more efficient without altering the basic operation. Low pressure ammonia vapor from the evaporator (4) is absorbed in the absorber by the solution. A pump circulates the strong solution (5-6) to the generator through the heat exchanger. In the generator, this solution (7) is boiled to release ammonia vapor by heat addition, leaving behind a weak solution (8), which is returned to the absorber (10) via a throttling valve to maintain the pressure differential between the high and low sides of the system. In the condenser, the ammonia vapor coming from the generator (1) is condensed to liquid (2). Then, it is passed via an expansion device to the evaporator pressure (3).

3. Modeling of the components

3.1 Assumptions

In the present study, in order to simplify the formulation and the consequent implementation of the model several conditions and assumptions were incorporated in the model without obscuring the basic physical situation. These conditions and assumptions were as follows:

a. The refrigerant leaving the evaporator and generator is at the state of saturated vapor.

b. The refrigerant leaving the condenser is at the state of saturated liquid.
c. There is no pressure loss in the pipes.
d. The fluid leaves each component at the component temperature.
e. The solutions leaving the various equipments are in the same concentration of the component inside.
f. The throttling valves between generator/absorber and condenser/evaporator are adiabatic.

3.2 Mathematical model

For the modelling of the absorption refrigeration system, the principles of mass conservation and the first and second laws of thermodynamics are applied to each component of the system. Each component can be treated as a control volume with inlet and outlet streams, heat transfer and work interactions. In the system, mass conservation includes the mass balance of each material of the solution. The governing equations of mass and type of material conservation for a steady-state, steady-flow system are [5]:

$$\sum \dot{m}_i - \sum \dot{m}_O \quad (1)$$

$$\sum (\dot{m} \cdot x)_i - \sum (\dot{m} \cdot x)_O \quad (2)$$

Where $\dot{m}$ is the mass flow rate and x is the mass concentration of NH_3 in the solution.

The first law of thermodynamics yields the energy balance of each component of the absorption system as follows [5]:

$$\sum (\dot{m} \cdot h)_i - \sum (\dot{m} \cdot h)_O + \left[\sum Q_i - \sum Q_O\right] + W = 0 \quad (3)$$

Where h is the specific enthalpy of working fluid at each corresponding state point, Q is the heat transfer and W is the pump work. In order to analyze the system in detail, mass and energy balance can be performed at each component.

At the generator, total mass balance, NH3 mass balance and energy balance are respectively calculated by using the following expressions:

$$\dot{m}_7 = \dot{m}_1 + \dot{m}_8 \quad (4)$$

$$x_7 \dot{m}_7 = x_1 \dot{m}_1 + x_8 \dot{m}_8 \quad (5)$$

$$\dot{m}_7 h_7 - \dot{m}_1 h_1 - \dot{m}_8 h_8 + Q_G = 0 \quad (6)$$

The heat responsible for the rise in the energy content in the generator derived from the solar collector is given by:

$$Q_G = U_G . A_G . (T_{HS} - T_G) \quad (7)$$

At the condenser, total mass and energy balances are calculated as follows;

$$\dot{m}_1 = \dot{m}_2 \quad (8)$$

$$\dot{m}_1 h_1 - \dot{m}_2 h_2 - Q_C = 0 \quad (9)$$

The heat rejected by the condenser can be calculated by:

$$Q_C = U_C . A_C . (T_C - T_{IS}) \quad (10)$$

At the evaporator, mass and energy balances are determined as follows:

$$\dot{m}_3 = \dot{m}_4 \quad (11)$$

$$\dot{m}_3 h_3 - \dot{m}_4 h_4 + Q_E = 0 \quad (12)$$

Such as cooling capacity produced is:

$$Q_E = U_E . A_E . (T_{CS} - T_E) \quad (13)$$

At the absorber, mass balance, refrigerant balance and energy balance are given as follows:

$$\dot{m}_5 = \dot{m}_4 + \dot{m}_{10} \quad (14)$$

$$x_5 \dot{m}_5 = x_4 \dot{m}_4 + x_{10} \dot{m}_{10} \quad (15)$$

$$\dot{m}_4 h_4 + \dot{m}_{10} h_{10} - \dot{m}_5 h_5 - Q_A = 0 \quad (16)$$

With the power rejected by the absorber is given by:

$$Q_A = U_A . A_A . (T_A - T_{IS}) \quad (17)$$

The process in the expansion device has been modeled as throttling in which enthalpy before and after the process has been assumed to be the same.

$$h_2 = h_3 = h_C \quad (18)$$

$$h_9 = h_{10} = h_{Ex} \quad (19)$$

The flows crossing the expansion valve V1 and V2 are function of the pressure difference upstream and downstream of the expander.

$$\dot{m}_2 = \omega_1 \sqrt{2.\rho_1 (HP - BP)} \quad (20)$$

$$\dot{m}_9 = \omega_2 \sqrt{2.\rho_2 (HP - BP)} \quad (21)$$

With:
ρ_1, ρ_1: density of the fluid upstream of the expander.
ω_1, ω_2: effective sections of the expansion valve.

In the pump, an incompressible strong solution and an average solution molar volume were assumed.

Based on these assumptions the pump power requirement is expressed as:

$$W_P = \dot{m}_5.\Delta P.V\left(x_5, T_5, HP\right) \quad (22)$$

The heat exchanger was treated as counter flow heat exchangers, which according to Niebergall [31] is the preferred flow configuration in absorption refrigeration systems. An energy balance calculation around the heat exchanger is given by:

$$\dot{m}_7\left(h_7 - h_6\right) = \dot{m}_8\left(h_8 - h_9\right) \quad (23)$$

The expression for the effectiveness is given as [32]:

$$\varepsilon = \frac{T_8 - T_9}{T_8 - T_6} \quad (24)$$

The COP for the system is usually defined as:

$$COP = \frac{Q_E}{Q_G + W_P} \quad (25)$$

3.3 Numerical implementation

The equation solver EES has been used to handle the resulting global model. To set up the global chiller model, all the individual component sets of equations have been linked together using internal variables, and the initial and external conditions have been specified.

4. Results and Discussion

Modeling of the system essentially implies prediction of the heat transfer for each of the system component, the COP of the system, the condition of all state points (Fig. 1) for the given physical dimensions of the plant and for the input conditions to the system (Table 1 and 2). As discussed earlier, this necessitates the determination of the operating conditions for which the mass and energy balances for the whole system are satisfied together with the performance characteristics of the individual component.

Table 1 Design parameters of the system

Element	Heat transfer area (m^2)	Overall heat transfer coefficient ($W\ m^{-2}\ K^{-1}$)
Generator	0.18	1500
Absorber	0.67	2500
Condenser	0.67	1500
Evaporator	0.8	700

Table 2 Set of input data used in the modeling

T_{HS} (K)	T_{IS} (K)	T_{CS} (K)	ε
400	303	278	0.8

4.1 The effects of the coefficient of performance

The effects of COP of main components on the key parameters of an absorption chiller namely T_A; T_G; T_C; T_E; Q_E; Q_G, mass flow, and pressure are investigated and shown in Figs. 2-6.

As it can be seen from Fig. 2, when the COP increases the generator temperatures increase. If the generator temperature gets higher, the thermal loads of the generator decreases, and hence, the COP increases, as it can be seen from Eqs. (7) and (22). Moreover, the evaporator temperature increases by the increasing of the COP. The absorber and condenser temperature decreases both by the decreasing the COP, and they rising from their initial value to the intermediate source temperature one.

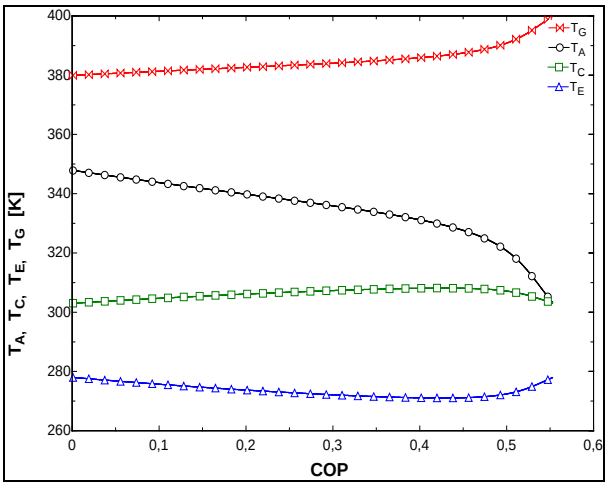

Fig. 2 The effect of COP on the components temperatures.

Fig. 3 shows the effect of the variation of the COP on the thermal loads of the generator and the evaporator components. QE passes through a maximum at the point COP = 0.41 and the maximum cooling capacity is Q_E = 6.893 kW. The coefficient of performance is relatively low since it can reach higher values. While the thermal loads Q_G decreases continuously. As it is seen from the Eq. (25), the performance of the cycle gets better with the decreasing of the generator thermal loads.

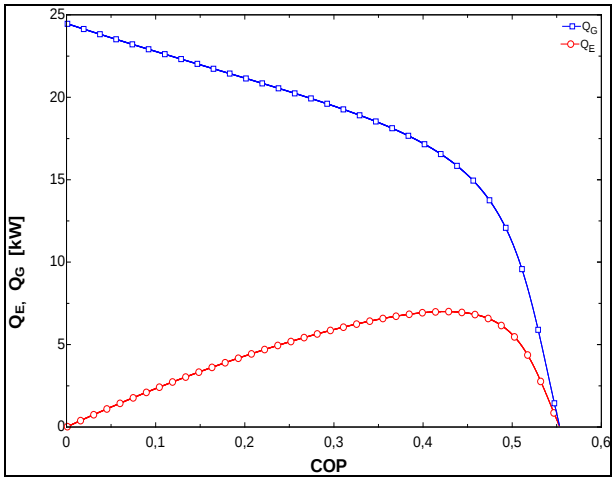

Fig. 3 The effect of COP on the generatorand evaporator heat load.

Fig. 4 shows the effect of COP on the flow of the strong and weak solution and ammonia flow. The ammonia flow responsible for the cooling effect has the same shape as that of the cooling capacity Q_E. The flow of the weak solution is slightly lower than the strong solution because the ammonia flow rate is relatively low. For the maximum refrigerating capacity, the flow rate of ammonia is 0.00673 kg/s.

Fig. 5 shows the effect of the variation of the COP on the mass fractions in the generator and the absorber. According to this figure, the increasing of the COP increases the gap between the two mass fractions. For the low COP, the flow rates of the weak and strong solutions are high; while the cooling effect is low (so $\dot{m}_{NH_3}$ is low) then the difference between the mass fractions is low. For the COP relatively large values, the gap between the mass fractions increases because the flow rate of solutions decreases and the cooling effect is relatively high.

Fig. 6 shows the variation of pressure levels depending on the COP. From this figure, we see that the low and high pressure passes respectively by a minimum and a maximum for COP = 0.41 which is the point where the cooling capacity is maximum.

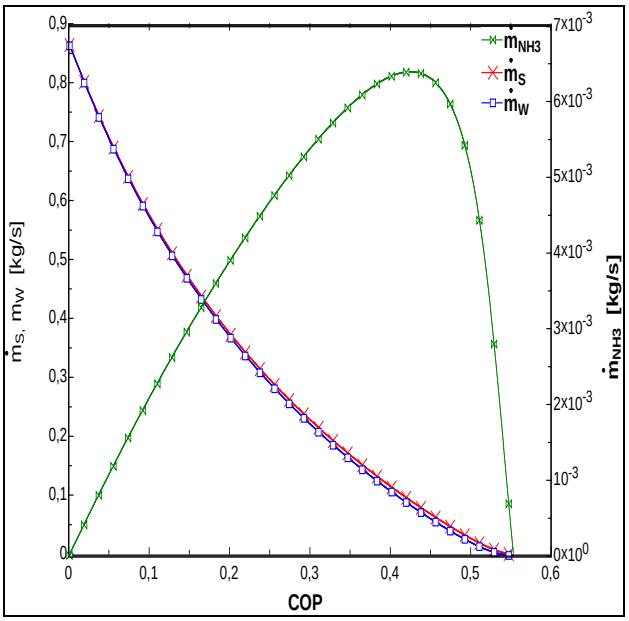

Fig. 4 The effect of COP on $\dot{m}_s, \dot{m}_w$ and $\dot{m}_{NH_3}$.

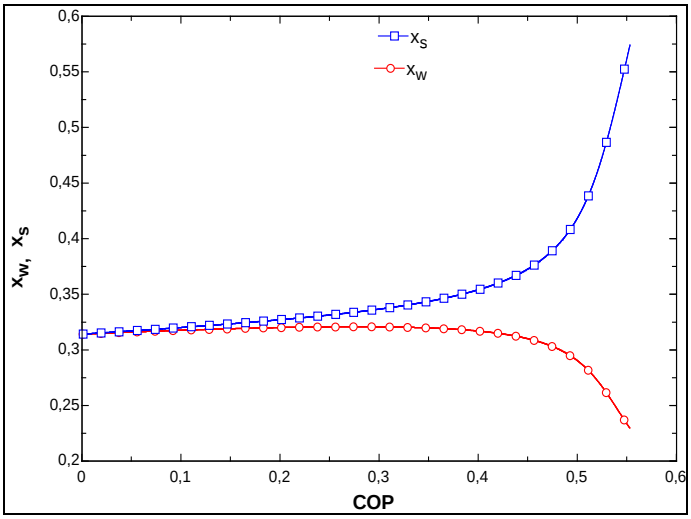

Fig. 5 The effect of COP on x_S and x_W.

The analysis of the different figures shows that the functional exchange area is for values greater than or equal to COP 0.41.

4.2 The effects of heat exchanger effectiveness

The effects of the heat exchanger on the thermal loads, performance of the system, mass flow rate and mass fraction are given in Figs. 7-11.

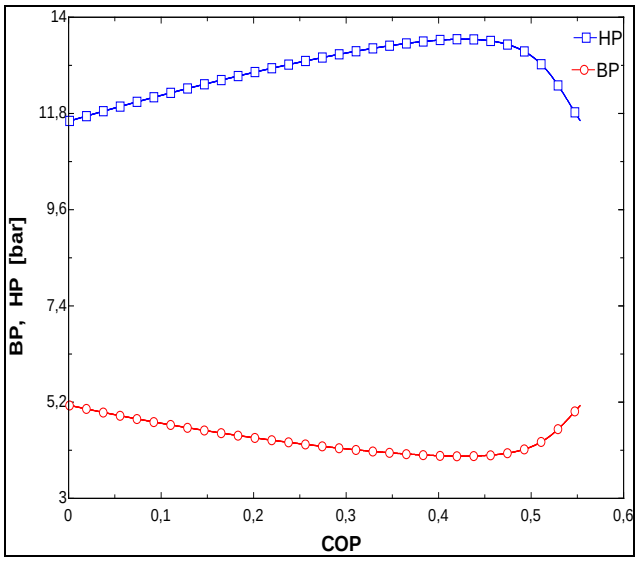

Fig. 6 The effect of COP on the on the pressure.

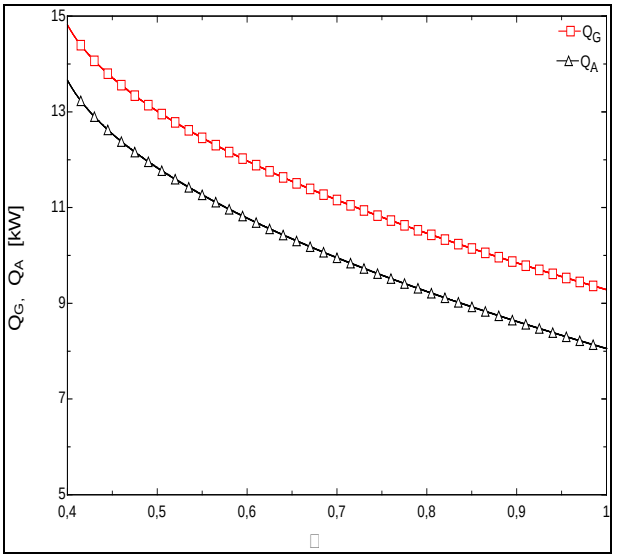

Fig. 7 The effect of the effectiveness of heat exchanger on the absorber and generator thermal load.

Fig. 7 and 8 shows the variation of the absorber, generator, evaporator and exchanger thermal loads with heat exchanger effectiveness. As known, if the effectiveness increases, the heat exchange between the weak and strong solutions increases, and as a result of this, the temperature of the weak solution (T9) decreases and that of the strong solution (T7) increases. With an increase in the strong solution temperature entering the generator, the heat load of the generator decreases. Similarly, with a decrease in the weak solution temperature entering the absorber, the heat rejected from the absorber also decreases. The evaporator thermal load increases with an increase in effectiveness of the heat exchanger, and hence, the COP increases as well.

The effects of the heat exchanger effectiveness on the system performance are given in Fig. 9. The performance of the system gets better with an increase in the effectiveness. For the best case condition ($\varepsilon = 1$, weak solution outlet temperature equals strong solution inlet temperature), the COP value increases up to a ratio of 55%.

For a fixed cooling load (Q_E = 6kW), increasing the heat exchanger efficiency involves a decrease in the mass flow of the strong and weak solution respectively.

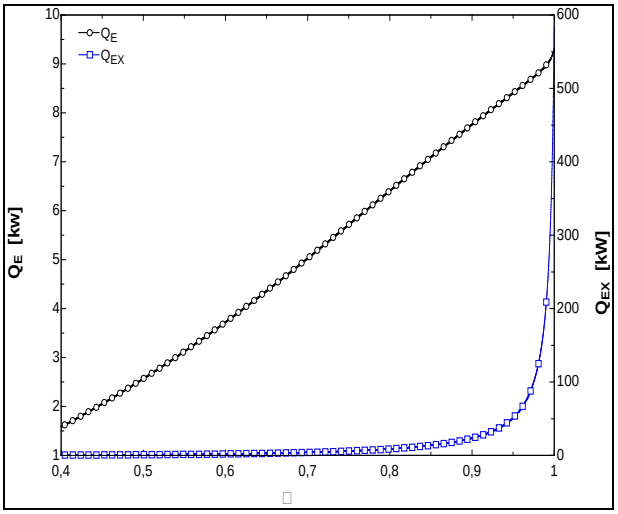

Fig. 8 The effect of the effectiveness of heat exchanger on the evaporator and exchanger thermal load.

This is explained by the fact that for increasing efficiency, so, increasing the temperature of the strong solution, need a smaller amount of the strong solution to desorb ammonia. And therefore decrease the mass flow of weak solution leaving the generator (Fig. 10).

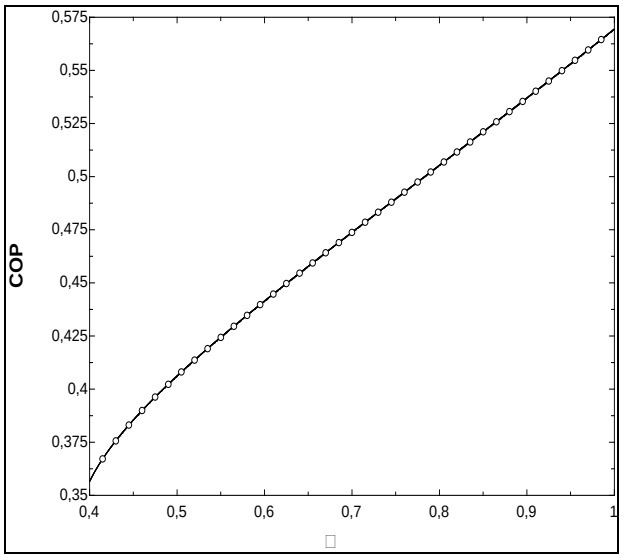

Fig. 9 The effect of the effectiveness of heat exchanger on the coefficient of performance.

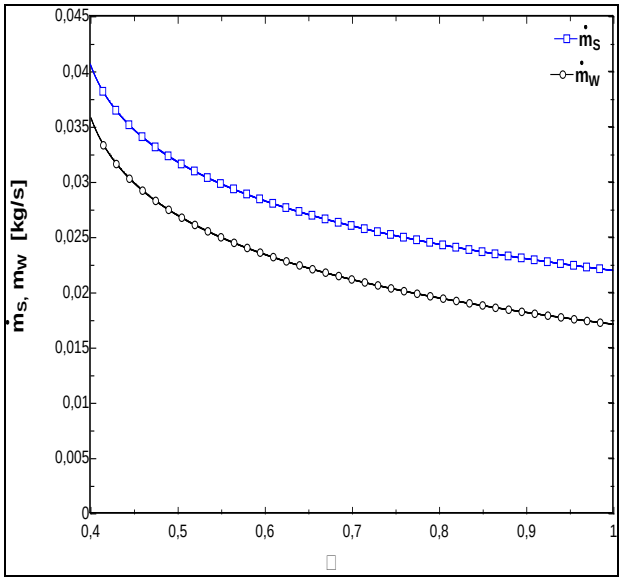

Fig. 10 The effect of the effectiveness of heat exchanger on the $\dot{m}_s$ and $\dot{m}_w$.

The increase of the heat exchanger efficiency increases the temperature of the generator hence it promotes the ammonia desorption and subsequently decreases the mass fraction of the lean solution. On the other hand, increasing the efficiency causes a decrease in the temperature of the absorber which promotes the absorption of ammonia and therefore the increase in the mass fraction of the rich solution (Fig. 11).

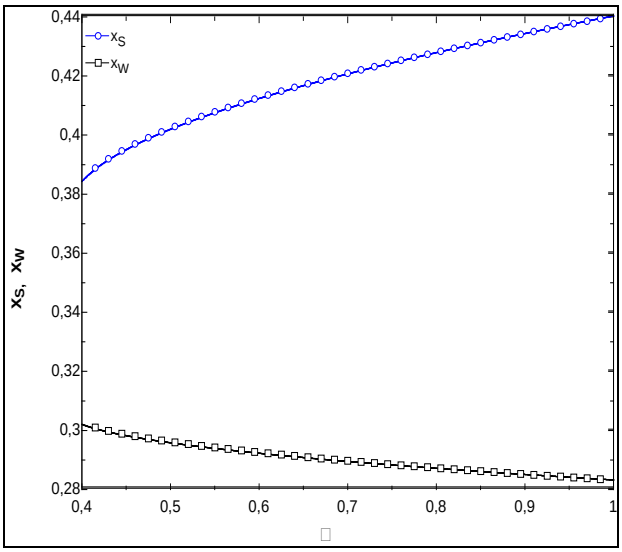

Fig. 11 The effect of the effectiveness of heat exchanger on the x_S and x_W .

5. Conclusion

In this study, simulation of an ammonia-water absorption refrigeration system, with detailed mass and heat transfer analysis has been carried out for air-conditioning application. From the above study, the following results can be drawn :

- The thermal loads of the evaporator and generator decrease, as the COP increase.
- The amount of ammonia vapor produced can reach 21 kg/h with the increasing of COP
- The increase of heat exchanger effectiveness increases the cooling capacity of the system to achieve for the best case condition (ε = 1) 9 kW.
- The increase of heat exchanger effectiveness increases the evaporator thermal loads. The maximum increase in the Q_E is of about 5%. Naturally, increasing Q_E, the COP increases in the same ratio. The COP increases from 0.36 to 0.57. In this case, the increase ratio in the COP is 55%.

References

[1] C. Koroneos, E. Nanaki, G. Xydis, Solar air conditioning systems and their applicability-an exergy approach, Resour. Conserv. Recycl. 55 (1) (2010) 74-82.

[2] C. Zhang, M. Yang, M. Lu, Y. Shan, J. Zhu, Experimental research on LiBr refrigeration-heat pump system applied in CCHP system, Appl. Therm. Eng. 31 n(17-18) (2011) 3706-3712.

[3] A. Sözen, M. Özalp, E. Arcaklioglu, Prospects for utilization of solar driven ejector-absorption cooling system in Turkey, Appl. Therm. Eng. 24 (2004) 1019-1035.

[4] O. Marc, J.P. Praene, A. Bastide, F. Lucas, Modeling and experimental validation of the solar loop for absorption solar cooling system using double-glazed collectors, Appl. Therm. Eng. 31 (2-3) (2011) 268-277.

[5] S.A. Kalogirou, Solar Energy Engineering: Process and Systems, first ed. Elsevier Ltd. Inc, New York, USA, (2009).

[6] X.Q. Zhai, R.Z. Wang, Experimental investigation and theoretical analysis of the solar adsorption cooling system in a green building, Appl. Therm. Eng. 29 (1) (2009) 17-27.

[7] D.S. Kim, C.A. Infante-Ferreira, Solar refrigeration options-a state-of-the-art review, Int. J. Refrig. 31 (1) (2008) 3-15.

[8] K. Bakirci, B. Yuksel, Experimental thermal performance of a solar source heat-pump system for residential heating in cold climate region, Appl. Therm. Eng. 31 (8-9) (2011) 1508-1518.

[9] V.G. Gude, N. Nirmalakhandan, Sustainable desalination using solar energy, Energy Convers. Manage. 51 (11) (2010) 2245-2251.

[10] R. Mastrullo, C. Renno, A thermoeconomic model of a photovoltaic heat pump, Appl. Therm. Eng. 30 (14-15) (2010) 1959-1966.

[11] F. Assilzadeh, S.A. Kalogirou, Y. Ali, K. Sopian, Simulation and optimization of a LiBr solar absorption cooling system with evacuated tube collectors, Renew. Energy 30 (8) (2005) 1143-1159.

[12] J. Sun, L. Fu, S. Zhang, W. Hou, A mathematical model with experiments of single effect absorption heat pump using LiBr-H2O, Appl. Therm. Eng. 30 (17-18) (2010) 2753-2762.

[13] J. Sun, L. Fu, S. Zhang, Performance calculation of single effect absorption heat pump using LiBr+LiNO3+H2O as working fluid, Appl. Therm. Eng. 30 (17-18) (2010) 2680-2684.

[14] J.R. García Cascales, F. Vera García, J.M. Cano Izquierdo, J.P. Delgado Marín, R. Martínez Sánchez, Modelling an absorption system assisted by solar energy, Appl. Therm. Eng. 31 (1) (2011) 112-118.

[15] B.H. Gebreslassie, G. Guillén-Gosálbez, L. Jiménez, D. Boer, Economic performance optimization of an absorption cooling system under uncertainty, Appl. Therm. Eng. 29 (17-18) (2009) 3491-3500.

[16] D. Hong, L. Tang, Y. He, G. Chen, A novel absorption refrigeration cycle, Appl. Therm. Eng. 30 (14-15) (2010) 2045-2050.

[17] C. Monné, S. Alonso, F. Palacín, L. Serra, Monitoring and simulation of an existing solar powered absorption cooling system in Zaragoza (Spain), Appl. Therm. Eng. 31 (1) (2011) 28-35.

[18] P. Srikhirin, S. Aphornratana, S. Chungpaibulpatana, A review of absorption refrigeration technologies, Renewable and Sustainable Energy Reviews 5 (4) (2001) 343–372.

[19] Y. Fan, L. Luo, B. Souyri, Review of solar sorption refrigeration technologies: Development and applications, Renewable and Sustainable Energy Reviews 11 (8) (2007) 1758–1775.

[20] N. A. Darwish, S. H. Al-Hashimi, A. S. Al-Mansoori, Performance analysis and evaluation of a commercial absorption–refrigeration water–ammonia (ARWA) system, International Journal of Refrigeration 31 (7) (2008) 1214-1223.

[21] J. C. Kapur, A report on the utilization of solar energy for refrigeration and air conditioning application. Sol Energy 4 (1) (1960) 39-47.

[22] E. A. Farber, F. M. Flanigan, L. Lopez, R. W. Polifka, Operation and performance of the University of Florida solar air-conditioning system. Sol Energy 10 (2) (1966) 91-95.

[23] M. R. Yeung, P. K. Yuen, A. Dunn, L. S. Cornish, Performance of a solar-powered air conditioning system in Hong Kong. Sol Energy 48 (5) (1992) 309-319.

[24] A. Syeda, M. Izquierdod, P. Rodríguez, G. Maidment, J. Missenden, A. Lecuona, R. Tozer, A novel experimental investigation of a solar cooling system in Madrid. Int J Refrig 28 (6) (2005) 859-71.

[25] F. Assilzadeh, S. A. Kalogirou, Y. Alia, K. Sopian, Simulation and optimization of a LiBr solar absorption cooling system with evacuated tube collectors. Renewable Energy 30 (8) (2005) 1143-1159.

[26] A. H Uppal, B. Norton, S. D. Probert, A low-cost solar-energy stimulated absorption refrigerator for vaccine storage, Appl Energy 25 (3) (1986) 167-174.

[27] M. D. Staicovici, An autonomous solar ammonia–water refrigeration system. Sol Energy 36 (2) (1986) 115-124.

[28] F. Z. Sierra, R. Best, F. A. Holland, Experiments on an absorption refrigeration system powered by a solar pond. Heat Recovery Syst CHP 13 (5) (1993) 401-408.

[29] M. Hammad, S. Habali, Design and performance study of a solar energy powered vaccine cabinet. Appl Therm Eng 20 (18) (2000) 1785-1798.

[30] A. De Francisco, R. Illanes, J. L. Torres, M. Castillo, M. De Blas, E. Prieto, A. Garcia, Development and testing of a prototype of low-power water–ammonia absorption equipment for solar energy applications. Renewable Energy 25 (4) (2002) 537-544.

[31] S.G. Alvares and Ch Trepp, Simulation of a solar driven aqua-ammonia absorption refrigeration system. Part 1: mathematical description and system optimization, Int. J. Refrig. 10 (1) (1987) 40-48.

[32] J. P. Holman Heat transfer, 8th ed. New York: McGraw Hill (1950).